Chin. Geogra. Sci. 2019 Vol. 29 No. 2 pp. 306–315
https://doi.org/10.1007/s11769-019-1030-6

Springer Science Press
www.springerlink.com/content/1002-0063

Changes in Global Cloud Cover Based on Remote Sensing Data from 2003 to 2012

MAO Kebiao[1, 2], YUAN Zijin[1], ZUO Zhiyuan[1], XU Tongren[2], SHEN Xinyi[3], GAO Chunyu[1]

(1. *National Hulunber Grassland Ecosystem Observation and Research Station*, *Institute of Agricultural Resources and Regional Planning*, *Chinese Academy of Agricultural Sciences*, *Beijing* 100081, *China*; 2. *State Key Laboratory of Remote Sensing Science*, *Institute of Remote Sensing and Digital Earth Research*, *Chinese Academy of Science and Beijing Normal University*, *Beijing* 100086, *China*; 3. *Hydrometeorology and Remote Sensing Laboratory*, *University of Oklahoma*, *Norman* 73072, *USA*)

Abstract: As is well known, clouds impact the radiative budget, climate change, hydrological processes, and the global carbon, nitrogen and sulfur cycles. To understand the wide-ranging effects of clouds, it is necessary to assess changes in cloud cover at high spatial and temporal resolution. In this study, we calculate global cloud cover during the day and at night using cloud products estimated from Moderate Resolution Imaging Spectroradiometer (MODIS) data. Results indicate that the global mean cloud cover from 2003 to 2012 was 66%. Moreover, global cloud cover increased over this recent decade. Specifically, cloud cover over land areas (especially North America, Antarctica, and Europe) decreased (slope = –0.001, R^2 = 0.5254), whereas cloud cover over ocean areas (especially the Indian and Pacific Oceans) increased (slope = 0.0011, R^2 = 0.4955). Cloud cover is relatively high between the latitudes of 36°S and 68°S compared to other regions, and cloud cover is lowest over Oceania and Antarctica. The highest rates of increase occurred over Southeast Asia and Oceania, whereas the highest rates of decrease occurred over Antarctica and North America. The global distribution of cloud cover regulates global temperature change, and the trends of these two variables over the 10-year period examined in this study (2003–2012) oppose one another in some regions. These findings are very important for studies of global climate change.

Keywords: global cloud cover; climate change; remote sensing; MODIS; global change

Citation: MAO Kebiao, YUAN Zijin, ZUO Zhiyuan, XU Tongren, SHEN Xinyi, GAO Chunyu, 2019. Changes in Global Cloud Cover Based on Remote Sensing Data from 2003 to 2012. *Chinese Geographical Science*, 29(2): 306–315. https://doi.org/10.1007/s11769-019-1030-6

1 Introduction

Global mean surface temperatures have increased by approximately 0.75℃ over the past century, and the mean decadal rate is approximately 0.13℃ (Rahmstorf and Coumou, 2011; Mao et al., 2017a). However, the trend in global surface temperatures has been nearly flat since the late 1990s, despite the continuous increases in the forcing that have occurred due to the total effects of well-mixed greenhouse gases (Solomon et al., 2010; Mao et al., 2017a; 2017b). Clouds are major regulators of Earth's radiation budget. They typically reflect more solar or shortwave (SW) radiation back to space than the Earth's surface, thus decreasing the energy retained within the Earth system, and they also usually emit less thermal infrared or longwave radiation to space than other bright surfaces, which decreases energy loss by the Earth. Cloud radiative forcing (CRF) is the difference between actual radiative flux and the radiative flux that would occur in the absence of clouds. SW-CRF is greatest for clouds with large albedo under strong insolation (Norris, 1999; Moore et al., 2001). Norris (1999) used synoptic

Received date: 2017-11-16; accepted date: 2018-03-14

Foundation item: Under the auspices of the National Key Project of China (No. 2018YFC1506602, 2018YFC1506502), National Natural Science Foundation of China (No. 41571427), the Anhui Natural Science Foundation (No. 1808085MF195), Open Fund of State Key Laboratory of Remote Sensing Science (No. OFSLRSS201708)

Corresponding author: MAO Kebiao. E-mail: maokebiao@caas.cn

surface cloud observations to examine interdecadal variability in global ocean cloud cover between 1952 and 1995. They found that total cloud cover over the ocean increased by 1.9% between 1952 and 1995. Hirakata (2014) made comparison of global and seasonal characteristics of cloud phase and horizontal ice plates derived from CALIPSO with MODIS and ECMWF.

Solomon et al. (2010) utilized the Bern 2.5CC intermediate complexity model to perform an analysis that was based mainly on the Halogen Occultation Experiment (HALOE) data sets. They found that stratospheric water vapor very likely contributed substantially to the flattening of the global warming trend after 2000, and the concentration of stratospheric water vapor decreased by approximately 10%, which acted to slow the rate of increase in global surface temperature from 2000 to 2009 in comparison with the increase that would have occurred given only the increases in CO_2 and other greenhouse gases (Solomon et al., 2010; Mao et al., 2017a; 2017b). Despite the key role that clouds play in the climate system, our understanding of the net response of clouds to climate change is still very limited. At present, it is not known whether changes in cloud cover, cloud reflectivity, and cloud height will mitigate or exacerbate global warming (Moore et al., 2001). The present study uses surface synoptic cloud observations obtained from the Extended Edited Cloud Report Archive (EECRA) to document variations in global ocean cloud cover during 1952–1997 and variations in global land cloud cover during 1971–1996 (Hahn and Warren, 1999).

The Moderate Resolution Imaging Spectroradiometer (MODIS) instruments are aboard the Terra and Aqua Earth Observing System (EOS) platforms, which were launched in December 1999 and May 2002. The MODIS atmospheric science team and other researchers developed a practical set of algorithms for cloud detection and the retrieval of cloud physical and optical properties (Gao and Kaufman, 1995; Ackerman et al., 1999; Platnick et al., 2003; Xia et al., 2015, 2018). The Cloud-Aerosol Lidar with Orthogonal Polarization (CALIOP) instrument provides detailed cloud and aerosol profile data that are often used to evaluate the accuracy of cloud-related property retrievals (Cho et al., 2008; Holz et al., 2008; Jethva et al., 2014). Significant improvements have been made to the MODIS cloud mask (MOD35 and MYD35) for Collection 5 reprocessing and forward stream data production. Most of the modifications were made for nighttime scenes, especially in polar and oceanic regions (Frey et al., 2008). The MODIS cloud mask uses a variety of cloud detection tests to indicate a level of confidence that MODIS is observing a clear-sky scene. The cloud mask algorithm uses up to 20 of the 36 MODIS spectral bands to maximize reliable cloud detections (Platnick et al., 2003), which are used to produce global day and night data products with a resolution of 1 km. The cloud mask essentially assesses the likelihood of a pixel being obstructed by clouds. As cloud cover can occupy different fractions of individual pixels, the MODIS cloud mask is designed to allow for varying degrees of clear-sky confidence. The archived results from the MODIS cloud detection algorithms have applications in climate change studies, climate modeling, and numerical weather prediction.

Clouds have a large impact on solar radiation and directly affect global temperature changes. Little research is available on changes in clouds globally. The main reason is that the cloud area is too large (the daily average cloud cover is nearly 70%), and changes in clouds occur too quickly, especially in remote areas such as oceans and deserts where changes in the clouds are difficult to monitor. The other reason is that the number of global cloud observation sites is relatively small, and the data collected at ground-based observation stations are frequently not representative. Cloud types also vary greatly among regions, depending on their latitudes and elevations. Although it is very difficult to analyze global changes in cloud cover using data obtained from meteorological stations because such local data do not represent large areas, the MODIS data provide an opportunity for us to carry out this work. In this study, the change of cloud area in different regions is analyzed using two MODIS sensors mounted on two satellites, which can help us understand cause of global surface temperatures change.

2 Data and Methods

NASA (National Aeronautics and Space Administration) has two polar-orbiting EOS (Earth Observation System) satellites (Terra and Aqua) in orbit at all times, with one satellite crossing the equator in the early morning (10:30) and early evening (22:30) and the other crossing the equator in the afternoon (13:30) and late evening (01:30). The Terra and Aqua satellites were launched by NASA in 1999 and 2002, respectively. They have sun-synchronous, near-polar orbits, which means that the satellites travel from the North Pole to the South Pole as the Earth rotates below them. The significance of a sun-synchronous orbit is that the satellite passes over the same part of Earth at

approximately the same local time each day, ensuring comparable daylight conditions over time. MODIS instruments are on board these two satellites. Together, they provide global cloud coverage estimates four times per day, and the resolution is 1 km × 1 km at nadir. Therefore, we can calculate global mean cloud cover from the MODIS data. The MODIS cloud products are archived into two categories: pixel-level retrievals (referred to as Level-2 products) and global gridded statistics at a latitudinal and longitudinal resolution of 1° (Level-3 products). The Level-3 products are temporally aggregated into daily, eight-day, and monthly files containing a comprehensive set of statistics and both marginal and joint probability distributions (Platnick et al. 2003).

Mao et al. (2016; 2017b) performed an analysis of global temperature and water vapor content and obtained many meaningful conclusions. Changes in cloud cover drive changes in global temperature and water vapor content. In this paper, we perform a similar analysis for global cloud cover and calculate global cloud cover from the MODIS cloud product MOD 03, which displays greater consistency for determining the distribution of changes in cloud cover. Equation (1) is used to compute the global mean cloud cover, similar to the estimation of global mean temperature and water vapor content (Mao et al., 2017a).

$$F_m = \frac{1}{n}\sum_{i=1}^{n}\sum_{j=1}^{l} S(j)\left(F_{ij}^{01:30} + F_{ij}^{10:30} + F_{ij}^{13:30} + F_{ij}^{22:30}\right) \Big/ 4 \quad (1)$$

where F_m is the mean cloud cover, n is the number of days in a year, l is the number of pixels, $S(j)$ is the area weighting function of pixel j and is obtained through the conversion of different coordinates, F_{ij} is the cloud cover on the ith day and within the jth pixel at the local time (01:30, 10:30, 13:30, 22:30) of day at the same location. Because no data are available from the Aqua satellite for 2001 and January–July 2002, we calculate the mean cloud cover in 2003. Equation (2) is used to estimate the rate of change of cloud cover from 2003 to 2012.

$$b = \frac{n\sum_{k=1}^{n}(k \times F_{mk}) - \sum_{k=1}^{n} k \sum_{k=1}^{n} F_{mk}}{n \times \sum_{k=1}^{n} k^2 - \left(\sum_{k=1}^{n} k\right)^2} \quad (2)$$

where b is the rate of change, k is the number of years, F_{mk} is the mean cloud cover in the kth year, and n is 10. In spatio-temporal analysis, Equation (3) is used to calculate the correlation coefficient (R) for each pixel.

culate the correlation coefficient (R) for each pixel.

$$R = \frac{n\sum_{k=1}^{n}(k \times F_{mk}) - \sum_{k=1}^{n} k \sum_{k=1}^{n} F_{mk}}{\sqrt{n \times \sum_{k=1}^{n} k^2 - \left(\sum_{k=1}^{n} k\right)^2} \times \sqrt{n \times \sum_{k=1}^{n} F_{mk}^2 - \left(\sum_{k=1}^{n} F_{mk}\right)^2}} \quad (3)$$

3 Results and Discussion

Statistical analyses on different regional scales are performed using Equation (1). The annual average cloud cover over ocean, land, and the globe from 2003 to 2012 are shown in Fig. 1. This figure indicates clearly that

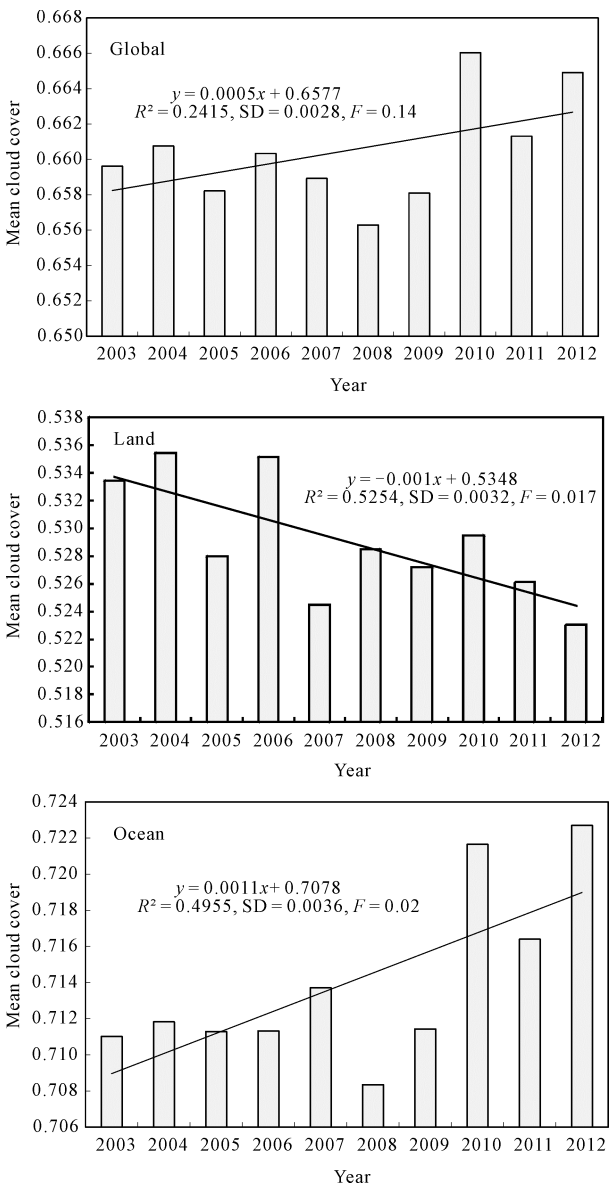

Fig. 1 Mean cloud cover of global, land and ocean from 2003 to 2012. SD: Standard Deviation

global mean cloud cover increased in 2010–2012. The global mean cloud cover is approximately 66%, and the years with the highest and lowest global mean cloud cover are 2010 and 2008, respectively. The mean cloud cover over land is 53%, and the years with the highest and lowest mean cloud cover over land are 2004 and 2012, respectively. The mean cloud cover over ocean areas is 71%, and the years with the highest and lowest mean cloud cover over ocean areas are 2012 and 2008, respectively. In Fig. 1, the mean cloud cover over land is decreasing, whereas it is increasing over the ocean.

The degree of cloud cover differs between the hemispheres, and the results are shown in Fig. 2. The mean cloud cover in the Northern Hemisphere is 63.5%, and the years with the highest and lowest mean cloud cover in the Northern Hemisphere are 2012 and 2009, respectively. The mean cloud cover in the Southern Hemisphere is 68.5%, and the years with the highest and lowest mean cloud cover in the Southern Hemisphere are 2010 and 2008, respectively. Fig. 2 indicates that cloud cover increased slightly in the two hemispheres during 2003–2012.

The mean cloud cover also differs over the seven continents, and the results are shown in Fig. 3. The mean cloud cover over Asia is 56.0%, and the years with the highest and lowest mean cloud cover over Asia are 2003 and 2009, respectively. The mean cloud cover over South America is 66.0%, and the years with the highest and lowest mean cloud cover are 2009 and 2010, respectively. The mean cloud over North America is 59.7%, and the years with the highest and lowest mean cloud cover over North America are 2004 and 2012, respectively. The mean cloud cover over Europe is 66%, and the years with the highest and lowest mean cloud cover over Europe are 2004 and 2011, respectively. The mean cloud cover over Antarctica is 38.4%, and the years with the highest and lowest mean cloud cover over Antarctica are 2004 and 2012, respectively. The mean cloud cover over Oceania is 38.0%, and the years with the highest and lowest mean cloud cover over Oceania are 2010 and 2005, respectively. The mean cloud cover over Africa is 40.7%, and the years with the highest and lowest mean cloud cover are 2006 and 2007, respectively. The analysis presented in Fig. 3 shows decreases in cloud cover over North America and Antarctica.

The cloud covers over four oceans are very different from continents (Fig. 4). The mean cloud cover over the Pacific Ocean is 72.4%, and the years with the highest and lowest mean cloud cover over the Pacific Ocean are 2012 and 2008, respectively. The mean cloud cover over the Indian Ocean is 71.6%, and the years with the highest and lowest mean cloud cover over the Indian Ocean are 2010 and 2006, respectively. The mean cloud cover over the Atlantic Ocean is 69.6%, and the years with the highest and lowest cloud cover over the Atlantic Ocean are 2011 and 2003, respectively. The mean cloud cover over the Arctic Ocean is 69.3%, and the years with the highest and lowest mean cloud cover are 2007 and 2004, respectively. This analysis indicates that the cloud cover over the Pacific and Indian Oceans increased slightly.

The spatial distribution of global mean cloud cover from 2003 to 2012 is shown in Fig. 5a. A linear regression has been performed for every pixel from 2003 to

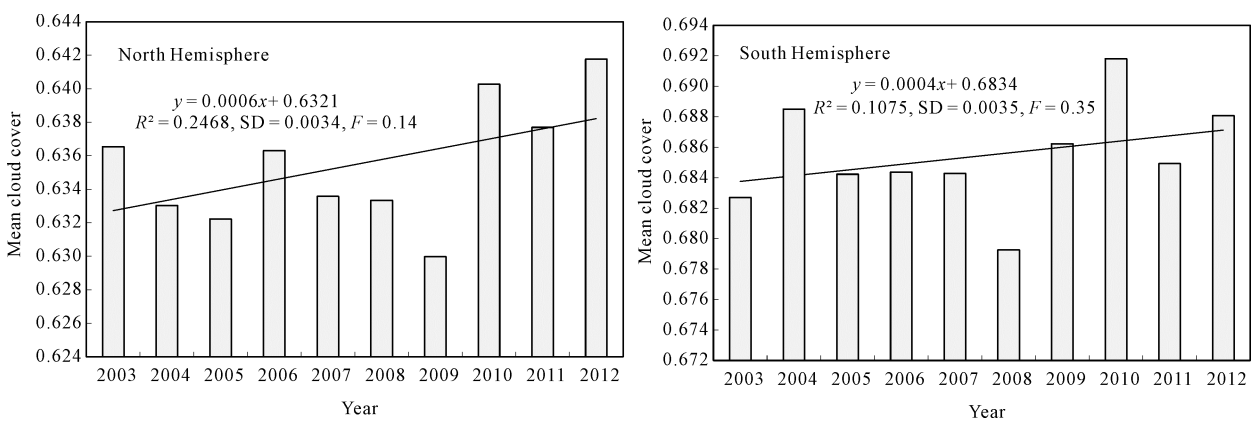

Fig. 2 Mean cloud cover in the Northern and Southern Hemispheres from 2003 to 2012

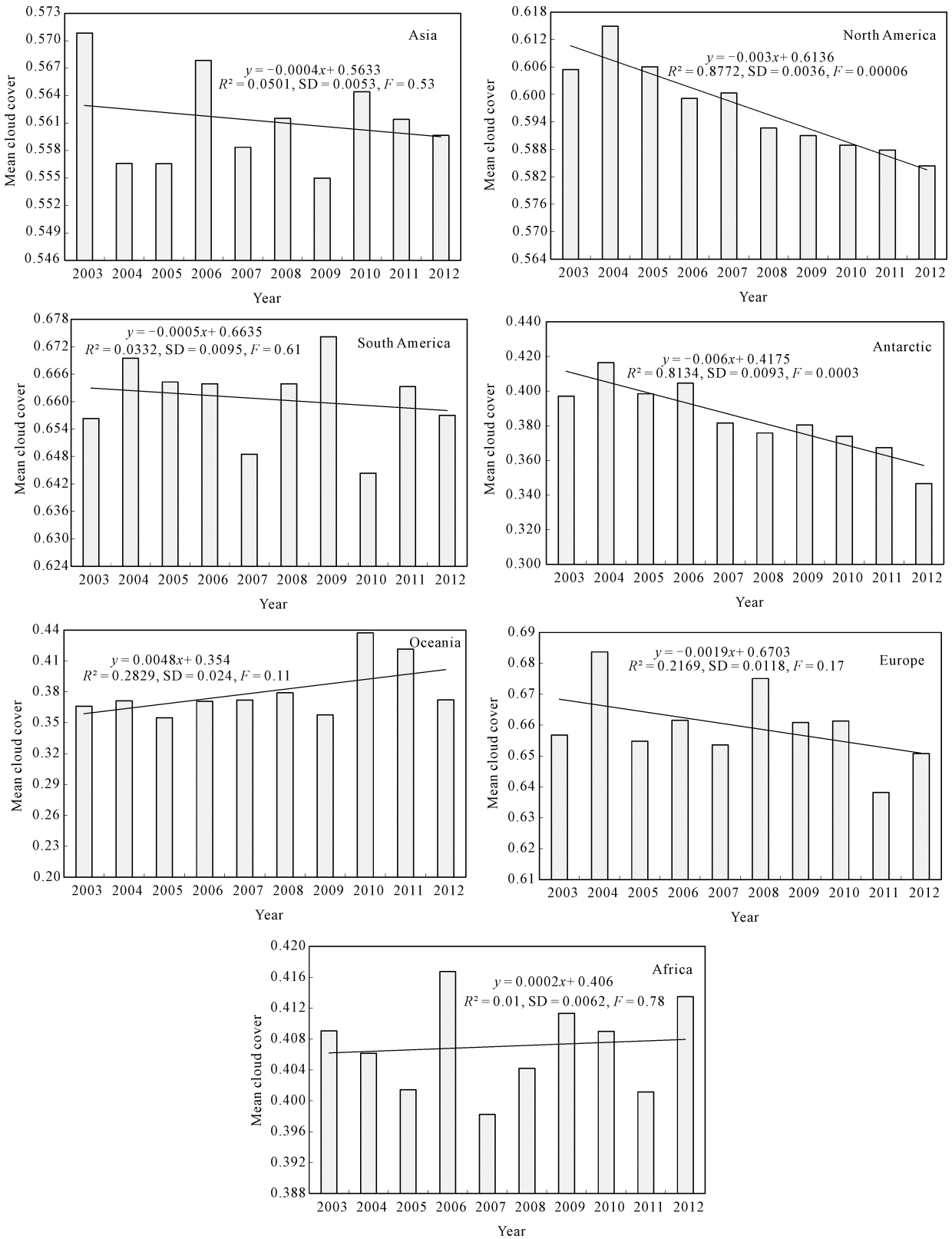

Fig. 3 Mean cloud cover over the seven continents from 2003 to 2012

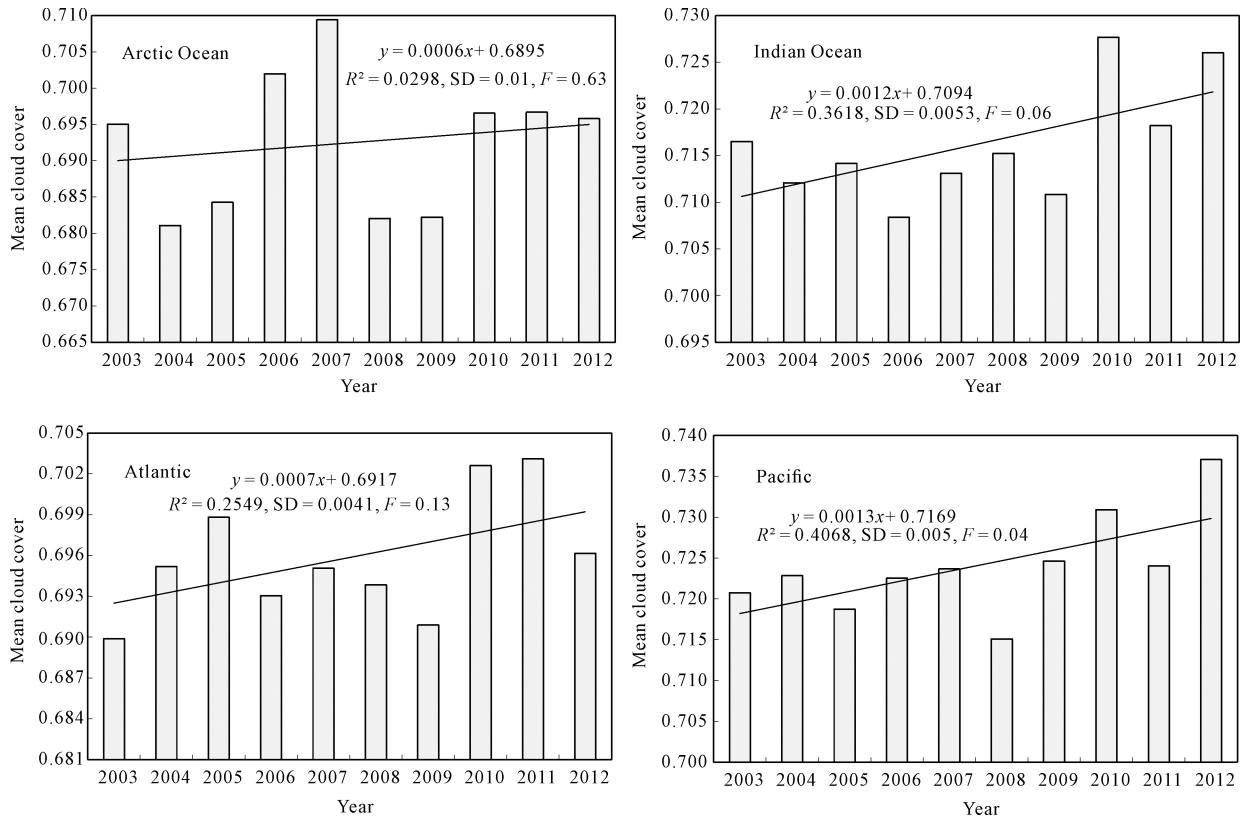

Fig. 4 Mean cloud cover over the four oceans from 2003 to 2012

2012, and Equation (2) is used to compute the rate of change of cloud cover (Fig. 5b). Fig. 5c shows a map of the correlation coefficient computed using Equation (3). The correlation coefficient is very high in places where the cloud cover changes greatly. As shown in Fig. 5a, the cloud cover between the latitudes of 36°S–68°S is relatively high compared to that in other regions, and the lowest cloud cover occurs in Oceania and Antarctica. The highest rates of increase occur over Southeast Asia and Oceania. The highest rates of decrease occur over Antarctica and North America. In the Pacific Rim region, cloud cover is relatively high, whereas it is relatively low in the Pacific Center. These findings are very important for studies of global climate change.

To analyze the change in cloud cover in the different seasons, we calculate the mean values for spring (March–May), summer (June–August), autumn (September–November), and winter (December–February) from 2003 to 2012. As shown in Fig. 6, the distribution of cloud cover changes with the season, especially in the Arctic and over Australia and North America. Cloud cover is lower in the Arctic in spring and winter than it is in summer and autumn.

The trends in global cloud cover by season are given in Fig. 7, and Fig. 8 shows a map of the correlation coefficient by season from 2003 to 2012. The cloud cover increases in summer in most regions, except Antarctica. The rate of change decreases over eastern North America in summer. The rate of change decreases over Antarctica in the spring, summer, and autumn, whereas it increases in winter. The trend in global cloud cover is the opposite of that in global surface temperature change (Mao et al., 2017b) over the 10 years examined in this study in most regions, and the spatial distribution of global cloud cover regulates global temperature and changes in water vapor content, which affects the spatial distribution of vegetation. The spatio-temporal variations in cloud cover also affect solar radiation, which regulates global surface temperature changes. Therefore, Mao et al. (2016; 2017a; 2017b) suggest that the influence of CO_2 on the Earth's temperature change is regulated by adjustments in the spatio-temporal distribution of clouds, changes in water vapor content, the release of geothermal heat from the seabed, ocean currents, and so on. The daily temperature changes of the Earth are determined by its rotation, and the temperature changes of the Earth from

spring to winter are due to the revolution of the Earth around the Sun. The inter-annul temperature changes of the Earth are determined by the movement of the other stars inside the solar system, and the longer period of temperature change is determined by the revolution of the solar system. Briefly, the temperature changes are mainly determined by the variations in the orbits of celestial bodies, and the changes in clouds play a role in mediating these changes (Mao et al., 2017a; 2017b).

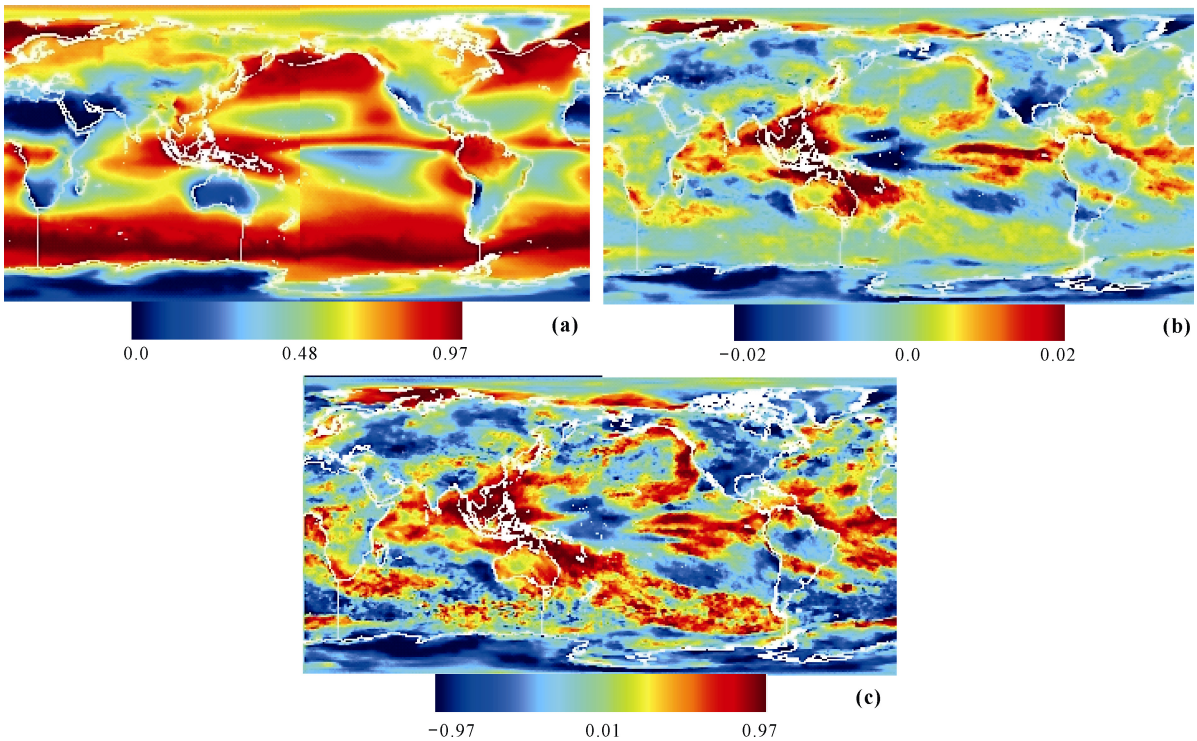

Fig. 5 Changes in global cloud cover from 2003 to 2012. (a) The annual mean; (b) rate (slope) of linear regression; (c) correlation coefficient computed by Equation (3).

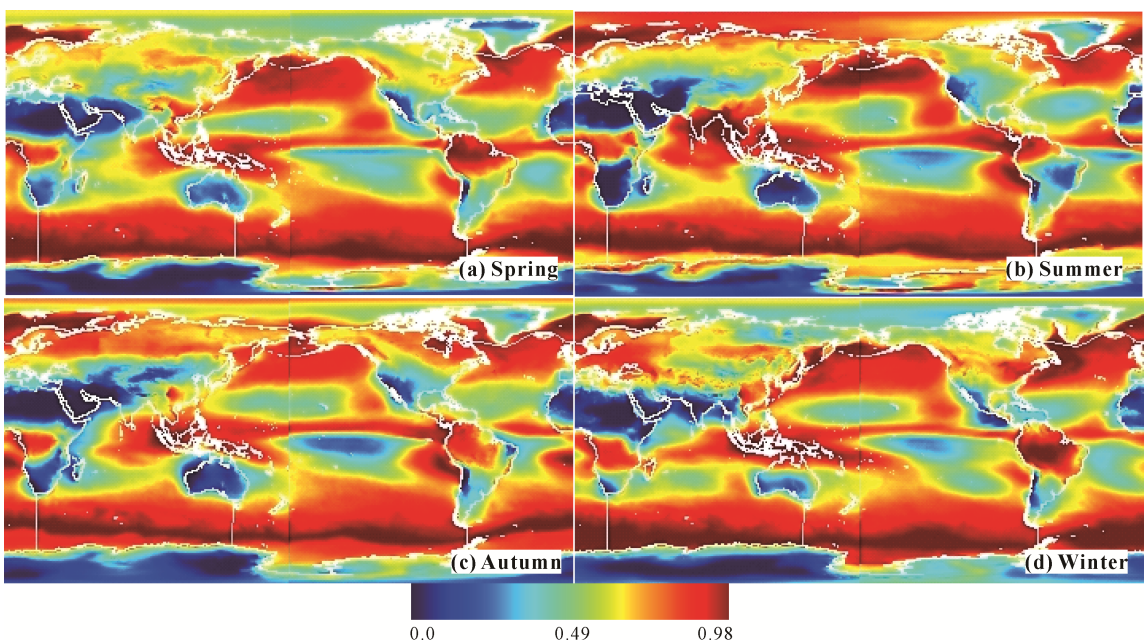

Fig. 6 Daily mean cloud cover from 2003 to 2012. (a) March–May; (b) June–August; (c) September–November; (d) December–February.

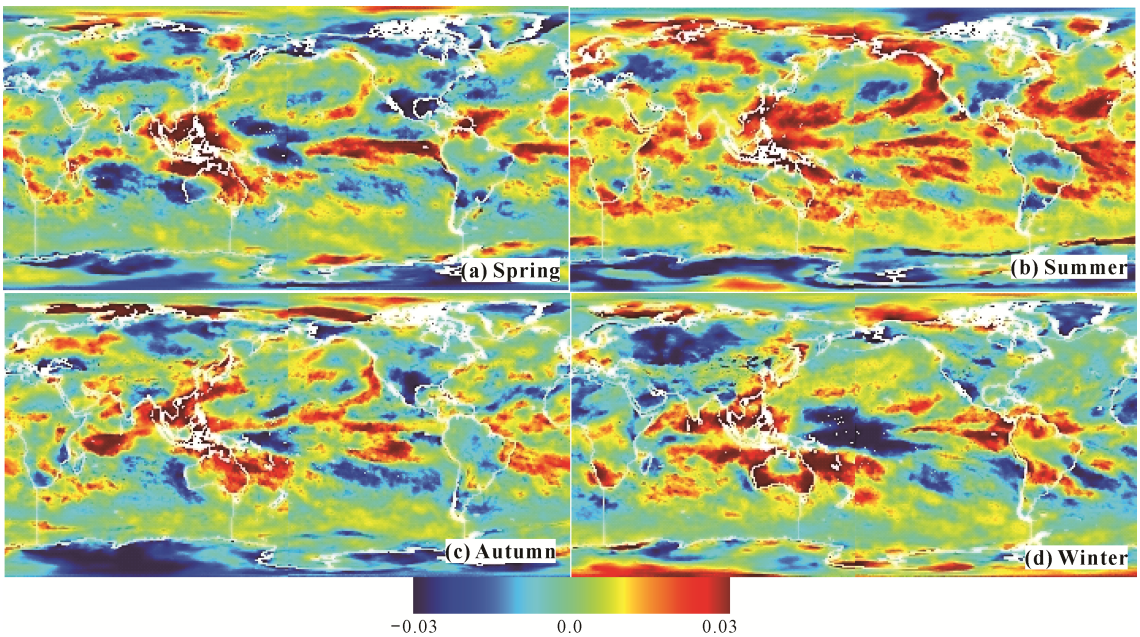

Fig. 7 Rate of change for cloud cover from 2003 to 2012, shown as the slopes of linear regressions. (a) March–May; (b) June–August; (c) September–November; (d) December–February.

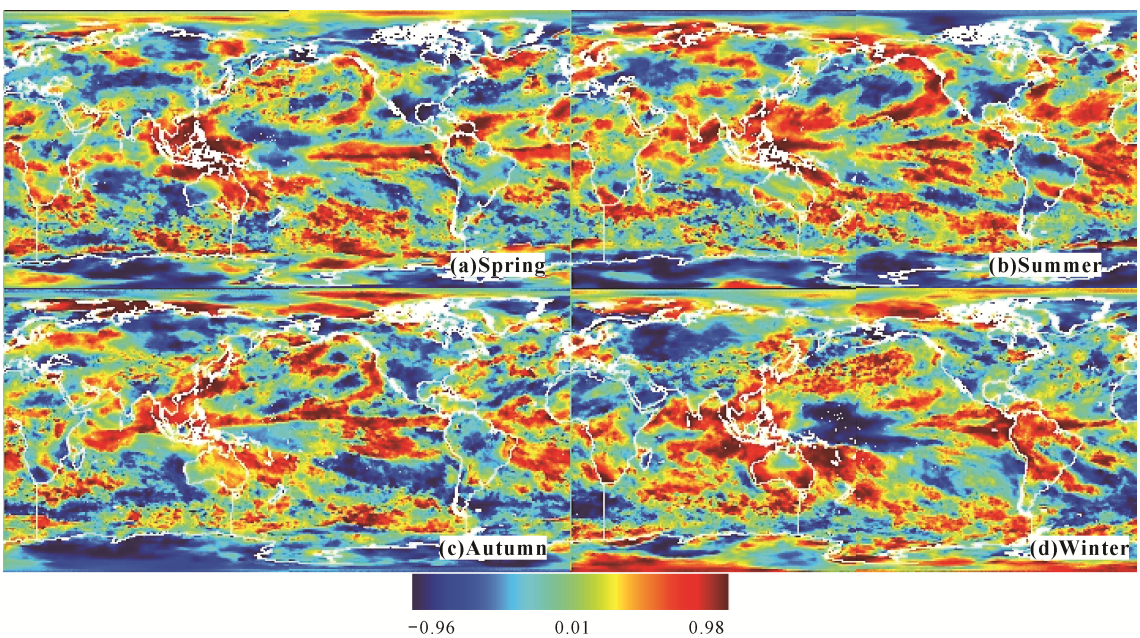

Fig. 8 The distribution of the correlation coefficient by season from 2001 to 2012. (a) March–May; (b) June–August; (c) September–November; (d) December–February.

4 Conclusions

Global mean cloud cover and surface temperature are not independent, which should satisfy the requirements of global energy balance. Cloud feedbacks in the climate system represent a major source of uncertainty in model projections of global warming. The atmospheric radiation budget is induced by changes in clouds that occur in response to climate forcing and dictate the eventual response of the global mean hydrological cycles of climate models to climate forcing. This linkage suggests that cloud feedbacks likely control the bulk precipitation efficiency and the associated responses of the hydrological cycle to radiative forcing of the climate system. This

paper offers an analysis of global cloud cover in recent years, and this comprehensive examination of cloud cover changes promises a holistic understanding of global climate change and the potential underlying mechanisms. Statistical analysis indicates that the global mean cloud cover from 2003 to 2012 was 66%. Moreover, global cloud cover increased over this recent decade; cloud cover over land areas (especially North America, Antarctica, and Europe) decreased (slope = –0.001, R^2 = 0.5254), whereas cloud cover over ocean areas (especially the Indian and Pacific Oceans) increased (slope = 0.0011, R^2 = 0.4955). Cloud cover is relatively high between the latitudes of 36°S and 68°S compared to other regions, and cloud cover is lowest over Oceania and Antarctica. Compared with other regions, and cloud cover is lowest over Oceania and Antarctica. The highest rates of increase occurred over Southeast Asia and Oceania, whereas the highest rates of decrease occurred over Antarctica and North America. These spatio-temporal variations in cloud cover may be a primary underlying cause of the change in the trend in global surface temperatures, which has been nearly flat since the late 1990s, and the effects of CO_2 have been offset by the spatial variations in cloud cover, which are mainly determined by the position of the Earth within the solar system and the galaxy. These findings are very important for the study of global climate-change. Furthermore, using more refined and updated data sets, these spatio-temporal variations can be examined, and they can be used in further analyses of climate change and the role of changes in cloud cover.

Acknowledgements

The authors thank the following persons for their help with this study: Anthony Arguez and Scott Stephens at NOAA's National Climatic Data Center.

References

Ackerman S A, Strabala K I, Paul M W et al., 1999. Discriminating clear sky from clouds with modis. *Journal of Geophysical Research*, 103(D24): 32141–32157. doi: 10.1029/ 1998JD 200032

Cho H, Yang P, Kattawar G W et al., 2008. Depolarization ratio and attenuated backscatter for nine cloud types: analyses based on collocated CALIPSO lidar and MODIS measurements. *Optics Express*, 16: 3931–3948. doi:10.1364/OE.16.003931

Frey R A, Ackerman S A, Liu Y H et al., 2008. Cloud detection with MODIS. Part I: improvements in the MODIS cloud mask for collection 5. *Journal of Atmosphere and Oceanic Technology*, 25(7): 1057–1072. doi:10.1175/2008JTECHA1052.1

Gao B C, Kaufman Y J, 1995. Selection of the 1.375-μm MODIS channel for remote sensing of cirrus clouds and stratospheric aerosols from space. *Journal of the Atmospheric Sciences*, 52(23): 4231–4237. doi:10.1109/IGARSS.2008.4780159

Hahn C J, Warren S G, 1999. Extended edited synoptic cloud reports from ships and land stations over the globe, 1952–1996. NDP026C, Carbon Dioxide Information Analysis Center, Oak Ridge National Laboratory, Oak Ridge, TN, 71. Available at: http://cdiac.esd.ornl.gov/epubs/ndp/ndp026c/ndp026c.html

Hirakata M, Okamoto H, Hagihara Y et al., 2014. Comparison of global and seasonal characteristics of cloud phase and horizontal ice plates derived from CALIPSO with MODIS and ECMWF. *Journal of Atmosphere and Oceanic Technology*, 31: 2114–2130. doi: http://dx.doi.org/10.1175/JTECH-D-13-00245.1

Holz R E, Ackerman S A, Nagle F W et al., 2008. Global Moderate Resolution Imaging Spectroradiometer (MODIS) cloud detection and height evaluation using CALIOP. *Journal of Geophysical Research*: *Atmospheres*, 113(D8): D00A19. doi: 10.1029/2008JD009837

Jethva H, Torres O, Waquet F et al., 2014. How do A-train sensors intercompare in the retrieval of above cloud aerosol optical depth? A case study-based assessment. *Geophysical Research Letters*, 41: 186–192. doi: 10.1002/2013GL058405

Mao K B, Li Z L, Chen J M et al., 2016. Global vegetation change analysis based on MODIS data in recent twelve years. *High Technology Letters*, 22(4): 343–349. doi:10.3773/j.issn. 10066748.2016.04.001

Mao K B, Ma Y, Tan X L et al., 2017b. Global surface temperature change analysis based on MODIS data in recent twelve years. *Advances in Space Research*, 59(2): 503–512. doi: 10. 1016/j.asr.2016.11.007

Mao Kebiao, Chen Jingming, Li Zhaoliang et al., 2017a. Global water vapor content decreases from 2003 to 2012: an analysis based on MODIS Data. *Chinese Geographical Science*, 27(1): 1–7. doi: 10.1007/s11769-017-0841-61

Moore III B, Gates W L, Mata L J et al., 2001. Advancing Our Understanding. In: Houghton J T et al. (eds.). *Climate Change 2001*: *The Scientific Basis*. Contribution of Working Group I to the Third Assessment Report of the Intergovernmental Panel on Climate Change. Cambridge: Cambridge University Press, 769–786.

Norris J R, 1999. On trends and possible artifacts in global ocean cloud cover between 1952 and 1995. *Journal of Climate*, 12(6): 1864–1870. doi: 10.1175/1520-0442(1999)012<1864: OTAPAI>2.0.CO;2

Norris J R, Wild M, 2007. Trends in aerosol radiative effects over Europe inferred from observed cloud cover, solar 'dimming', and solar 'brightening'. *Journal of Geophysical Research*: *Atmospheres*, 112(D8): D08214. doi: 10.1029/2006JD007794

Platnick S, King M D, Ackerman S A et al., 2003. The MODIS cloud products: algorithms and examples from terra. *IEEE Transactions on Geoscience and Remote Sensing*, 41(2): 459–473. doi: 10.1109/TGRS.2002.808301

Rahmstorf S, Coumou D, 2011. Increase of extreme events in a

warming world. *Proceedings of the National Academy of Sciences of the United States of America*, 108(44): 17905–17909. doi: 10.1073/pnas.1101766108

Solomon S, Rosenlof K H, Portmann R W et al., 2010. Contributions of stratospheric water vapor to decadal changes in the rate of global warming. *Science*, 327(5970): 1219–1223. doi: 10.1126/science.1182488

Steven P, Michael D K, Steven A A, et al., 2003. The MODIS cloud products: algorithms and examples from Terra. *IEEE Transactions on Geoscience and Remote Sensing*, 41(2): 459–473. doi: 10.1109/TGRS.2002.808301

Xia L, Zhao F, Chen L et al., 2018. Performance comparison of the MODIS and the VIIRS 1.38μm cirrus cloud channels using libRadtran and CALIOP data. *Remote Sensing of Environment*, 206: 363–374. doi: https://doi.org/10.1016/j.rse.2017.12.040

Xia L, Zhao F, Ma Y et al., 2015. An improved algorithm for the detection of cirrus clouds in the Tibetan Plateau using VIIRS and MODIS data. *Journal of Atmosphere and Oceanic Technology*, 32 (11): 2125–2129. doi:10.1175/JTECH-D-15-0063.1